Accepted Manuscript

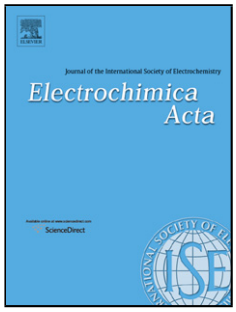

Title: Self-discharge of AC/AC electrochemical capacitors in salt aqueous electrolyte

Author: L. García-Cruz P. Ratajczak J. Iniesta V. Montiel F. Béguin

PII: S0013-4686(16)30731-9
DOI: http://dx.doi.org/doi:10.1016/j.electacta.2016.03.159
Reference: EA 26989

To appear in: *Electrochimica Acta*

Received date: 28-1-2016
Revised date: 25-3-2016
Accepted date: 26-3-2016

Please cite this article as: L.García-Cruz, P.Ratajczak, J.Iniesta, V.Montiel, F.Béguin, Self-discharge of AC/AC electrochemical capacitors in salt aqueous electrolyte, Electrochimica Acta http://dx.doi.org/10.1016/j.electacta.2016.03.159

Self-discharge of AC/AC electrochemical capacitors in salt aqueous electrolyte

L. García-Cruz[1,2], *P. Ratajczak*[1], *J. Iniesta*[2+], *V. Montiel*[2], *F. Béguin*[1*].

[1]Institute of Chemistry and Technical Electrochemistry, Poznan University of Technology, Berdychowo 4, 60-965 Poznan, Poland.

[2] Institute of Electrochemistry, University of Alicante, E-03080 Alicante, Spain.

Abstract

The self-discharge (SD) of electrochemical capacitors based on activated carbon electrodes (AC/AC capacitors) in aqueous lithium sulfate was examined after applying a three-hour cell potential hold at U_i values from 1.0 to 1.6 V. The leakage current measured during the potentiostatic period as well as the amplitude of self-discharge increased with U_i; the cell potential drop was approximately doubled by 10°C increase of temperature. The potential decay of both negative and positive electrodes was explored separately, by introducing a reference electrode and it was found that the negative electrode contributes essentially to the capacitor self-discharge. A diffusion controlled mechanism was found at $U_i \leq 1.4$ V and $U_i \leq 1.2$ V for the positive and negative electrodes, respectively. At higher U_i of 1.6 V, both electrodes display an activation controlled mechanism due to water oxidation and subsequent carbon oxidation at the positive electrode and water or oxygen reduction at the negative electrode.

Keywords: Self-discharge, AC/AC electrochemical capacitor, aqueous lithium sulfate electrolyte, diffusion-controlled mechanism, activation-controlled mechanism.

---

* Corresponding author. Tel.: +48 61 647 5985.
E-mail address: francois.beguin@put.poznan.pl (F. Béguin).
ISE Member.

1. Introduction

The use of organic electrolytes in electrochemical capacitors (ECs) has been considered for long time as the best option to achieve the high cell potential values (2.7 – 2.8 V) which are desirable for obtaining high energy density [1]. However, organic solvents present several disadvantages such as toxicity, environmental unfriendliness and high cost. Besides, basic or acidic aqueous electrolytes are environmentally friendly, enabling to reach higher capacitance and lower electrical resistance than organic electrolytes, but the cell potential is generally limited to less than 1 V [2]. Neutral aqueous electrolytes are an interesting alternative to organic solutions as they allow achieving higher operating cell potential than traditional aqueous electrolytes, e.g., KOH or H_2SO_4. Good cycle life was reported up to cell potential as high as 1.6 V and 1.9 V for activated carbon (AC)-based ECs in aqueous Na_2SO_4 (0.5 mol L^{-1}) [3] and Li_2SO_4 (2 mol L^{-1}) [4], respectively. Such high operating cell potential is owing firstly to the high over-potential for di-hydrogen evolution at the negative electrode [5, 6], and secondly to the less corrosive character of neutral electrolyte as compared to, e.g., H_2SO_4, thus allowing the development of these electrochemical devices with non-noble metals for current collectors. The maximum cell potential of ECs using neutral aqueous electrolyte is essentially limited by the positive electrode which potential may exceed the electrochemical stability limit of water oxidation, leading to irreversible reactions, such as electrolyte decomposition, formation of oxygenated functional groups on the carbon surface and corrosion of the underlying stainless steel collector [7, 8]. Furthermore, when the porosity of activated carbon electrodes fits appropriately with the electrolyte ions size, EC capacitance can be improved. Therefore, in an effort to

understand the relationship between carbon porosity and EC performance in neutral aqueous electrolytes, it is extremely important to take into account the effect of polymer binder applied for electrodes preparation [7-9].

Apart from capacitance and resistance evolution during cycling of ECs, the self-discharge (SD) of ECs, i.e., the potential decay which occurs when the cell is set to opened circuit after being charged, is a parameter of major interest for applications. As it is well known in the literature, a charged capacitor is in a state of high free energy relative to the discharged state, so there is a thrust force for self-discharge [10]. The phenomenon of SD of an electrochemical capacitor diminishes its performance characteristics, namely power density and energy density. Hence, SD is one of the most important and relevant issues [11-13] which needs to be minimized, and a profound knowledge of SD mechanisms as well as its control is vital for the improvement of ECs [10, 14]. The SD rate is defined by the mechanistic route which governs the discharge phenomena [15, 16]. In this regard, Conway described the different SD mechanisms and derived kinetic models which aid to predict the SD profile and to explain the related phenomena [10].

According to literature, the SD of ECs might be due to charge redistribution, and the carbon pore shape has a significant influence on this mechanism [17, 18]. Indeed, due to the resistance of the electrolyte confined in the carbon porosity, pores of different geometries are charged at different rates, and charge redistribution from higher to lower surface charge density areas takes place in the porosity at open circuit after charging. Also, internal ohmic leakage currents generated by a faulty construction and Faradaic reactions with either activation or diffusion controlled mechanism might be the causes

of SD process [11, 15, 19, 20]. Activation controlled SD takes place with high concentration species such as electrolyte or functionality on the carbon surface. In that case, the plot of cell potential decay *vs* logarithm of time displays as a plateau followed by a linear drop of potential. Besides, diffusion-controlled SD is related with faradaic reactions of low concentration species, i.e. impurities present either in the electrolyte or in carbon electrodes or any other capacitor component. The latter are metal ions shuttles, which can be oxidized/reduced at one electrode, and then diffuse under the imposed electrostatic field to the other electrode where they are reduced/oxidized [21]. Moreover, in the case of deoxygenated solution with remaining low concentration of di-oxygen and/or di-hydrogen, the Nernstian potentials can be modified and water be consequently oxidized/reduced giving rise to SD [16, 22]. For a diffusion-controlled faradaic process, a linear cell potential drop with square root of time is obtained. In either activation or diffusion controlled mechanism, the leakage current depends on the initial cell potential ($U_{i.}$).

For ECs based on symmetric carbon electrodes and aqueous electrolyte, water electrolysis and oxygen reduction have been proposed as possible redox reactions which may cause the SD of a capacitor [12]. Water electrolysis involves both O_2 and H_2 evolution on the positive and negative electrodes, respectively. However, it has been demonstrated that in a symmetric carbon/carbon capacitor, the evolution of both gases from water electrolysis is not the direct cause of SD [12]. Besides, the study of negative electrode SD at 0.0 V, in absence and presence of di-oxygen in the bulk solution by bubbling either nitrogen or oxygen gas, revealed that an increment of oxygen concentration caused a significant potential drop with time of the negative electrode at

open circuit, in addition to a diffusion-controlled SD; hence, it is likely that O_2 reduction on the negative electrode is the main cause of SD [12]. As already demonstrated in the literature, SD depends on parameters such as temperature, maximum cell potential reached and hold time at this value, and the charge/discharge history [20, 23]. To date, the majority of studies were focused on SD dependence with the kind of aqueous electrolyte , in absence [6, 24-27] or presence of certain surfactants [26, 27] or redox couple (redox-active electrolyte) [28], and type of separator [24, 29].

This work explores the SD profiles of AC/AC electrochemical capacitors in lithium sulfate neutral aqueous solution, with the aim of understanding the mechanisms and further finding strategies to reduce SD. Capacitors SD as well as of individual negative and positive electrodes was analyzed at various values of cell potential hold (U_i) and temperature.

2. Experimental

2.1 *Chemicals and materials*

The activated carbon DLC Supra 30 (further named AC) was kindly provided by Norit, and acetylene black C65 (AB) by Imerys. The binder was polytetrafluoroethylene (PTFE, 60 wt.% dispersion in water from Sigma Aldrich). Lithium sulfate monohydrate was purchased from Sigma Aldrich (≥ 99.0% purity). Ethanol and acetone were purchased from Sigma Aldrich (≥99.5% purity). All chemicals and solvents were employed as received without any further purification. All aqueous solutions were prepared with ultrapure deionized water (18.2 MΩ cm).

2.2 Electrodes preparation

PTFE-based electrodes (AC-PTFE) were prepared by mixing 80 wt.% of AC, 10 wt.% of electrically conductive percolator AB and 10 wt.% of PTFE polymer binder, as described elsewhere [9]. Briefly, all materials mentioned above were mixed in such amount to obtain a total mass of 0.2 g in ca. 20 mL of ethanol 96 % v/v. Then, the mixture was heated at 70ºC with continuous magnetic stirring until ethanol was evaporated to reach a homogeneous composite. Subsequently, a few drops of ethanol were mixed with the carbon composite until obtaining dough. Next, the carbon dough was rolled into a thin carbon sheet with a thickness between ca. 0.110 mm and 0.170 mm. Thereafter, the rolled carbon dough was dried under vacuum at 120 ºC for 12 h and then cooled down to room temperature. Finally, circular pellets were punched out from the dried dough sheet, with an apparent geometric area of 0.785 cm^2 (ca. 4 mg) for Swagelok-type cells and 1.539 cm^2 (ca. 12 mg) for coin cells.

2.3 Porous texture analysis of electrodes by nitrogen adsorption.

The nitrogen adsorption isotherms at 77 K of the materials were obtained with an ASAP 2020 (Micromeritics). Prior to the sorption analyses, the AC pristine powder was degassed under vacuum at 350°C for 24 h, whereas the electrodes were degassed at 140 ºC for 24 h. The specific surface area was determined by application of the BET equation. All porous texture data of electrodes were referred to the mass of active carbon material. Table 1 summarizes the textural parameters of the pristine AC powder and AC-PTFE electrode.

Table 1. Textural parameters of as-received AC powder and AC-PTFE electrode. [a]Total pore volume evaluated at relative pressure of 0.99 from the N_2 adsorption isotherms at 77K. [b]Micropore and mesopore volume evaluated from the Dubinin-Radushkevich (DR) method applied to the N_2 adsorption isotherms. [c]Average micropore size L_0 determined from the Stoeckli equation: L_0 (nm) = 10.8/(E_0 - 11.4 kJ mol^{-1}) where E_0 is the characteristic energy of the DR equation [30].

	BET specific surface area [$m^2 \cdot g^{-1}$]	V_{total} [$cm^3 \cdot g^{-1}$][a]	V_{micro} < 2 [nm] [$cm^3 \cdot g^{-1}$][b]	V_{meso} [$cm^3 \cdot g^{-1}$][b]	Average micropore size (L_0) < 2 [nm][c]
AC pristine	2066	1.100	0.908	0.172	1.54
AC-PTFE	1835	1.00	0.807	0.156	1.55

2.4 Self-discharge experiments

SD of the electrochemical capacitors was measured using CR 2025 coin cells (from MTI) consisting of a stainless steel case, with seal O-ring, a stainless steel spacer (0.2 mm thickness), and a stainless steel wave spring (0.3 mm thickness). Two-electrode Teflon Swagelok-type cells with Hg/Hg_2SO_4; K_2SO_4 (0.5 mol L^{-1}) reference electrode (E_0 = 0.680 V vs NHE) were used to monitor simultaneously the cell SD and the potential variation of the individual negative and positive electrodes. Both types of cells were built with 2.0 mol L^{-1} lithium sulfate electrolytic solution in deionized water (pH = 6.5), and the electrodes were separated by absorptive glass matt (AGM, 0.52 mm thickness) kindly provided by Bernard Dumas. The amount of electrolyte used was comparable in both coin cells and Swagelok cells, only to soak the electrodes and the separator, without any excess and flooding.

The electrochemical measurements were performed using a VMP3 multichannel potentiostat-galvanostat (Biologic, France) on coin cells at 24 ± 1 ºC and 34 ± 1 ºC and on Swagelok-type cells at 24 ± 1 ºC, using a climatic chamber (SML 25/250 ZALMED, Poland). Before measuring SD, the cells were cycled between 0 and 0.8 V by cyclic voltammetry at a scan rate of 5 $mV \cdot s^{-1}$, in order to reach repeatable steady-state voltammograms. For SD experiments, the cells were charged at 200 $mA \cdot g^{-1}$ from the open circuit cell potential to the desired U_i (1.0, 1.2, 1.4 or 1.6 V) which was further held for 3 h (process called floating), during which the current response (so-called leakage current) was recorded *vs* time. After 3 h of potentiostatic period at the demanded U_i, the electrochemical capacitor was disconnected from the power supply (open circuit) and the potential of cell (and electrodes) was recorded for 15 h.

3. Results and discussion

3.1 Self-discharge dependence with initial cell potential

In preliminary experiments, ECs were charged to a given potential, U_i, which was held for either 2 h or 3 h, after which the SD profiles were recorded under open circuit conditions. Since both profiles did not demonstrate significant differences, a hold time of 3 h at given U_i was considered to be long enough to enable potential equalization and charge redistribution in all pores of the activated carbon electrodes [15]. As shown in table 1, the usage of PTFE binder enables to reduce the loss of pore volume while keeping the average pore size unchanged. Consequently, the porosity of the activated carbon electrode fits well with the size of ions and allows them to move easily through unobstructed access.

Figure 1 displays the plots of cell potential *vs* time for an AC-PTFE /AC-PTFE coin cell in 2.0 mol L^{-1} Li_2SO_4 after 3 h of floating at different values of U_i. It can be observed that the cell potential decreases to reach an almost constant value after 15 h of SD. The decline of cell potential is moderate, ca. 0.2 V, for U_i of 1.0 V and 1.2 V, respectively, and it becomes more significant at U_i = 1.4 and 1.6 V. Similarly, faster decrease of open circuit cell potential voltage was reported for commercial supercapacitors in acetonitrile-based electrolyte when the cells had been charged to a higher initial potential [20]. The plots of leakage current recorded during the floating period at various U_i (figure 2) show comparable values for U_i = 1.0 V and 1.2 V and a noticeable increase throughout all floating time when U_i > 1.2 V. The use of a high electrolyte concentration, such as 2.0 mol L^{-1}, ensures that the diffusion of ions throughout the AC electrode is not limited by their availability, especially at high cell potential [31]. Hence, the more significant leakage current and SD of the EC at higher U_i might be attributed to faradaic reactions related with water electrolysis when the cell potential exceeds the thermodynamic value of 1.23 V, namely: (i) overcharging and corrosion of the positive stainless steel collector [7, 8]; (ii) reaction of the formed oxygen within the electrolyte solution or creation of functionalities on the surface of activated carbon, leading even to pore blockage during floating [7, 32]; iii) other side faradaic reactions due to some impurities [21, 22]. Recently, Abbas et al. [9] have measured the potential range of electrodes *vs* cell potential of a carbon/carbon symmetric EC with AC-PTFE electrodes of same composition in neutral aqueous electrolyte, and have proved that the potential of the AC-PTFE positive electrode exceeds the thermodynamic limit of water oxidation at cell potential of 1.4 V. Hence,

oxygen evolution and carbon oxidation [7] are likely important causes of the enhanced SD and leakage current at U_i > 1.4 V in our experiments; it will be further proved by analysis of the SD profiles, demonstrating activation controlled mechanism at U_i > 1.4 V.

3.2 Effect of temperature on self-discharge

Figure 3 shows the SD of the AC-PTFE/AC-PTFE cell in 2.0 mol L^{-1} Li_2SO_4 at 34°C after 3 h of floating. The comparison of the SD profiles at 24 ºC and 34 ºC (Figures 1 and 3) reveals that the cell potential drop is higher by ca. 50 mV at 34°C for U_i ranging from 1.0 to 1.4 V, and by ca. 125 mV for U_i = 1.6 V; at the end of self-discharge at 34 ºC, the cell potential is almost the same for U_i = 1.4 V and 1.6 V. Moreover, the higher values of leakage current at 34°C for $U_i \geq$ 1.4 V, and more particularly for U_i = 1.6 V (Figure 4), confirm faradaic side reactions activated by an increase of temperature, i.e. water electrolysis, corrosion, oxidation of carbon, for which the current is utilized [7]. Hence, these side reactions have a detrimental effect on the performance of ECs based on AC electrodes in lithium sulfate aqueous electrolyte, particularly at higher temperature.

Notwithstanding, at $U_i \leq$1.2 V, it is likely that the increase of SD with temperature is not related with faradaic causes but to the intrinsic properties of the EDL. Indeed, SD of an electrochemical capacitor is a kinetic process, which is therefore influenced by temperature according to the Arrhenius equation [10]:

$$I(T) = A \exp(-E_a / RT) \qquad (1)$$

where I (T) denotes the self-discharge current, T the temperature in Kelvin, R the gas constant R = 8.31451 J mol^{-1} K^{-1}, A a pre-exponential factor and E_a the activation energy. Equation (1) allows explaining the effect of faster SD at all U_i by increasing the storage temperature from 24 to 34°C. Conway indicated that effectively for every 10ºC temperature increase, the SD rate is doubled for a capacitor with a typical activation energy value of 40 kJ mol^{-1} [10]. It also explains the increase of leakage current value with temperature during floating at $U_i \leq 1.4$ V (compare figures 2 and 4).

To better elucidate the SD mechanism depending on U_i, the SD profiles of the AC-PTFE/AC-PTFE coin cell capacitor in 2.0 mol L^{-1} lithium sulfate at 34°C have been analysed *vs* $t^{1/2}$ and ln t (Figure 5). The linear dependence of U *vs* $t^{1/2}$ for U_i values of 1.0 and 1.2 V (Figure 5a), where faradaic reactions do not take place, reveals a diffusion controlled process [19] due to the presence of impurities and/or dissolved gas. An increase of temperature favors the diffusion of the latter from the bulk solution to the electrodes surface, where if a suitable cell potential is reached, oxidation or reduction reactions can easily take place. At U_i = 1.4 V, the SD profile seems to be mixed diffusion/activation controlled. By contrast at U_i = 1.6 V, the U *vs* $t^{1/2}$ plot is no longer linear and the SD profile is better described by an activation-controlled faradaic process (figure 5b), where the U *vs* ln t curve displays a plateau followed by a linear potential decay [13]. In sum, the SD mechanism at 34°C is essentially diffusion controlled till 1.2 V and it shifts to activation controlled at U_i >1.4 V.

According to [33], assuming a first order reaction with respect to the charge Q, an apparent rate constant, k_{app}, for the self-discharge reaction can be evaluated through equation (2):

$$dQ/dt = - k_{app} Q \quad (2)$$

which then can be transformed into (3) for a typical EDL cell:

$$dU/dt = - k_{app} U \quad (3)$$

which after integration gives:

$$\ln U = \ln U_i - k_{app}t \quad (4)$$

where U_i is the initial cell potential. Hence, for the two temperatures T_1 = 297K (24°C) and T_2 = 307K (34°C) and for each value of U_i (1.0, 1.2, 1.4 and 1.6 V), the plot of ln U *vs* t is linear, and enables the values of k_{app1} and k_{app2} reported in table 2 to be determined from the slope. Then, for each value of U_i, the temperature dependence of the apparent rate constant can be fitted to the Arrhenius equation:

$$\ln k_{app}(T) = \ln A - E_a / RT \quad (5)$$

and the values of activation energy estimated (see table 2) from the k_{app} values obtained at the two temperatures T_1 and T_2 as follows:

$$E_a = - R \ln (k_{app2}/k_{app1}) / (T_2^{-1} - T_1^{-1}) \quad (6)$$

Table 2. Values of apparent rate constant at 24°C and 34ºC and of activation energy for various values of initial cell potential. AC-PTFE/AC-PTFE coin cells in 2.0 mol L^{-1} lithium sulfate.

Initial Cell Potential (U_i) / V	Rate constant (k_{app1})/ s^{-1} at 24ºC	Rate constant (k_{app2})/ s^{-1} at 34ºC	Activation energy (E_a)/ kJ mol^{-1}
1.0	1.32 x 10^{-5}	1.83 x 10^{-5}	25
1.2	1.66 x 10^{-5}	2.47 x 10^{-5}	30
1.4	2.64 x 10^{-5}	3.92 x 10^{-5}	30
1.6	4.16 x 10^{-5}	7.65 x 10^{-5}	46

At U_i = 1.0 V, where we have identified diffusion controlled SD, the E_a value of 25 kJ mol^{-1} is close to the range of 16-20 kJ mol^{-1} previously reported for such kind of process [10]. Similarly, the value of 46 kJ mol^{-1} at U_i = 1.6 V is also in agreement with the literature data of 40-80 kJ mol^{-1} for an activation controlled mechanism [10]. For U_i = 1.4 V, the value of 30 kJ mol^{-1} confirms mixed diffusion/activation controlled SD, as suggested by figure 5. Hence, the mechanism may be different at both electrodes, therefore it would be worth to analyze separately SD of the individual electrodes; this will be the object of the next section.

3.3 Self-discharge behavior of positive and negative electrodes.

The evolution of cell potential, as well as the potential of the positive and negative electrodes separately, was explored by introducing an Hg/Hg_2SO_4; K_2SO_4 (0.5 mol L^{-1}) reference electrode in the AC-PTFE/AC-PTFE cell. The SD profiles reveal that the negative electrode is essentially responsible of SD whatever U_i value, and the difference between ΔE_- and ΔE_+ increases with U_i (figure 6, table 3). Taking into account our previous data displaying that, at high cell potential, the lowest potential of the negative electrode is lower than the water reduction potential [6], it is obvious that higher SD of this electrode is related with water reduction, as it will be further demonstrated in figure 8 by its activation controlled characteristics at $U_i \leq 1.4$ V. In addition, since SD measurements were realized with non-deoxygenated aqueous electrolyte, oxygen electrochemical reduction to hydrogen peroxide (at -0.3 V vs NHE at pH = 6.5) is surely another cause of negative electrode SD, as already demonstrated by Andreas in [12].

Table 3. Cell potential drop and positive and negative electrode potential variation after self-discharge of AC-PFTE/AC-PTFE cells in 2.0 mol L^{-1} lithium sulfate during 3 hours. Storage temperature 24 ± 1 ºC.

Initial Cell Potential (U_i) / V	Positive electrode potential variation ΔE^+ / V	Negative electrode potential variation ΔE^- / V	Cell potential drop ΔU / V
1.0	0.059	0.078	0.137
1.2	0.079	0.108	0.187
1.4	0.116	0.167	0.283
1.6	0.188	0.279	0.467

The plots of cell and electrodes potential variation *vs* $t^{½}$ and ln t are shown in figure 7 and 8, respectively. Considering the positive electrode, the E_+ *vs* $t^{1/2}$ plots are fairly linear up to U_i = 1.4 V (Figure 7b), confirming a diffusion controlled mechanism. At U_i = 1.6 V, the E_+ *vs* ln t plot is typical of an activation controlled mechanism, with and initial plateau followed by a linear decay. At such U_i, the potential of the positive electrode is higher than the water oxidation limit leading to oxygen evolution and carbon oxidation [7,9]. Considering now the negative electrode, the E_- *vs* $t^{1/2}$ plots are linear for U_i = 1 and 1.2 V (figure 7), confirming a diffusion controlled mechanism. At higher value of U_i (1.4 V and 1.6 V), the mechanism shifts to an activation-controlled faradaic one since, in the E_- *vs* ln t plot, the potential decay is linear after a plateau region (Figure 8c). As pointed out before, water reduction and O_2 reduction to H_2O_2 may take place from U_i = 1.4 V, being responsible of negative electrode and EC activation-controlled self-discharge.

4. Conclusions

The presented study disclosed that, after potential hold of an AC/AC capacitor in 2.0 mol L^{-1} Li_2SO_4, the negative electrode is mainly responsible of self-discharge at all values of U_i, though the contribution of the positive electrode cannot be neglected. A diffusion controlled mechanism due to impurities is observed up to U_i = 1.4 V for the positive electrode and U_i = 1.2 V for the negative one. At $U_i \geq 1.4$ V, the potential of the negative electrode becomes lower than either water or dissolved oxygen reduction potential, causing activation controlled SD. In the case of the positive electrode, the potential becomes higher than the water oxidation limit at U_i close to 1.6 V, causing carbon oxidation and appearance of activation controlled SD.

Hence, these findings revealed that faradaic processes of different nature at each electrode may contribute to the self-discharge of the electrochemical capacitor. Therefore, to understand the causes of capacitor self-discharge and determine strategies for its reduction, it was extremely important to analyze separately the potential decay of each electrode. Future works will be now dedicated to reduce Faradaic processes taking place at the positive electrode by reducing the maximum potential of the positive electrode. For the negative electrode, blocking hydroxyl anions in the porosity by designing pores with bottleneck entrances could be a way to reduce the pH changes and to keep overpotential conditions, even in absence of external polarization.

Acknowledgements

The authors are grateful to the Foundation for Polish Science (FNP) for funding the ECOLCAP project within the WELCOME program, co-financed from European

Union Regional Development Fund. LGC acknowledges the Spanish MINECO for funding her PhD mobility grant EEBB-1-13-06222 for the research stay at Poznan University of Technology. Norit, Imerys and Bernard Dumas are acknowledged for providing the carbon materials and separator used in this study.

References

[1] F. Béguin, V. Presser, A. Balducci, E. Frackowiak, Carbons and Electrolytes for Advanced Supercapacitors, Adv. Mater. 26 (2014) 2219.
[2] V. Ruiz, R. Santamaría, M. Granda, C. Blanco, Long-term cycling of carbon-based supercapacitors in aqueous media, Electrochim. Acta 54 (2009) 4481.
[3] L. Demarconnay, E. Raymundo-Pinero, F. Béguin, A symmetric carbon/carbon supercapacitor operating at 1.6 V by using a neutral aqueous solution, Electrochem. Commun. 12 (2010) 1275.
[4] Q. Gao, L. Demarconnay, E. Raymundo-Pinero, F. Béguin, Exploring the large voltage range of carbon/carbon supercapacitors in aqueous lithium sulfate electrolyte, Energ. Environ. Sci. 5 (2012) 9611.
[5] S.-E. Chun, J.F. Whitacre, Investigating the role of electrolyte acidity on hydrogen uptake in mesoporous activated carbons, J. Power Sources 242 (2013) 137.
[6] Q. Abbas, P. Ratajczak, P. Babuchowska, A. Le Comte, D. Bélanger, T. Brousse, F. Béguin, Strategies to Improve the Performance of Carbon/Carbon Capacitors in Salt Aqueous Electrolytes, J. Electrochem. Soc. 162 (2015) A5148.
[7] P. Ratajczak, K. Jurewicz, F. Béguin, Factors contributing to ageing of high voltage carbon/carbon supercapacitors in salt aqueous electrolyte, J. Appl. Electrochem. 44 (2014) 475.
[8] P. Ratajczak, K. Jurewicz, P. Skowron, Q. Abbas, F. Béguin, Effect of accelerated ageing on the performance of high voltage carbon/carbon electrochemical capacitors in salt aqueous electrolyte, Electrochim. Acta 130 (2014) 344.
[9] Q. Abbas, D. Pajak, E. Frackowiak, F. Béguin, Effect of binder on the performance of carbon/carbon symmetric capacitors in salt aqueous electrolyte, Electrochim. Acta 140 (2014) 132.
[10] B.E. Conway, Electrochemical Supercapacitors: Scientific fundamentals and Technological Applications, New York 1999.
[11] J. Black, H.A. Andreas, Prediction of the self-discharge profile of an electrochemical capacitor electrode in the presence of both activation-controlled discharge and charge redistribution, J. Power Sources 195 (2010) 929.
[12] A.M. Oickle, H.A. Andreas, Examination of Water Electrolysis and Oxygen Reduction As Self-Discharge Mechanisms for Carbon-Based, Aqueous Electrolyte Electrochemical Capacitors, J. Phys. Chem. C 115 (2011) 4283.
[13] H.A. Andreas, J.M. Black, A.A. Oickle, Self-discharge in Manganese Oxide Electrochemical Capacitor Electrodes in Aqueous Electrolytes with Comparisons to Faradaic and Charge Redistribution Models, Electrochim. Acta 140 (2014) 116.
[14] F. Béguin, E. Frackowiak, Supercapacitors: Materials, Systems, and Applications, Wiley, Weinheim (2013).

[15] J. Black, H.A. Andreas, Effects of charge redistribution on self-discharge of electrochemical capacitors, Electrochim. Acta 54 (2009) 3568.
[16] B.E. Conway, W.G. Pell, T.C. Liu, Diagnostic analyses for mechanisms of self-discharge of electrochemical capacitors and batteries, J. Power Sources 65 (1997) 53.
[17] J. Niu, B.E. Conway, W.G. Pell, Comparative studies of self-discharge by potential decay and float-current measurements at C double-layer capacitor and battery electrodes, J. Power Sources 135 (2004) 332.
[18] J.M. Black, H.A. Andreas, Pore Shape Affects Spontaneous Charge Redistribution in Small Pores, J. Phys. Chem. C 114 (2010) 12030.
[19] J.W. Graydon, M. Panjehshahi, D.W. Kirk, Charge redistribution and ionic mobility in the micropores of supercapacitors, J. Power Sources 245 (2014) 822.
[20] J. Kowal, E. Avaroglu, F. Chamekh, A. S'Enfelds, T. Thien, D. Wijaya, D.U. Sauer, Detailed analysis of the self-discharge of supercapacitors, J. Power Sources 196 (2011) 573.
[21] H.A. Andreas, K. Lussier, A.M. Oickle, Effect of Fe-contamination on rate of self-discharge in carbon-based aqueous electrochemical capacitors, J. Power Sources 187 (2009) 275.
[22] B. Pillay, J. Newman, The influence of side reactions on the performance of electrochemical double-layer capacitors, J. Electrochem. Soc. 143 (1996) 1806.
[23] M. Kaus, J. Kowal, D. U. Sauer, Modelling the effects of charge redistribution during self-discharge of supercapacitors, Electrochim. Acta 55 (2010) 7516.
[24] C. Libin, B. Hua, H. Zhifeng, L. Lei, Mechanism investigation and suppression of self-discharge in active electrolyte enhanced supercapacitors, Energ. Environ. Sci. 7 (2014) 1750.
[25] S.Y. Wang, N.L. Wu, Operating characteristics of aqueous magnetite electrochemical capacitors, J. Appl. Electrochem. 33 (2003) 345.
[26]] K. Fic, G. Lota, E. Frackowiak, Electrochemical properties of supercapacitors operating in aqueous electrolyte with surfactants, Electrochim. Acta 55 (2010) 7484.
[27] K. Fic, G. Lota, E. Frackowiak, Effect of surfactants on capacitance properties of carbon electrodes, Electrochim. Acta 60 (2012) 206.
[28] S.-E. Chun, B. Evanko, X. Wang, D. Vonlanthen, X. Ji, G.D. Stucky, S.W. Boettcher, Design of aqueous redox-enhanced electrochemical capacitors with high specific energies and slow self-discharge, Nat. Commun. 6 (2015) 7818.
[29] X.-Z. Sun, X. Zhang, B. Huang, Y.-W. Ma, Effects of Separator on the Electrochemical Performance of Electrical Double-Layer Capacitor and Hybrid Battery-Supercapacitor, Acta Physico-Chim. Sin. 30 (2014) 485.
[30] F. Stoeckli, M.V. Lopez-Ramon, D. Hugi-Cleary, A. Guillot, Micropore sizes in activated carbons determined from the Dubinin-Radushkevich equation, Carbon 39 (2001) 1115.
[31] W.G. Pell, B.E. Conway, N. Marincic, Analysis of non-uniform charge/discharge and rate effects in porous carbon capacitors containing sub-optimal electrolyte concentrations, J. Electroanal. Chem. 491 (2000) 9.
[32] K. Kierzek, E. Frackowiak, G. Lota, G. Gryglewicz, J. Machnikowski, Electrochemical capacitors based on highly porous carbons prepared by KOH activation, Electrochim. Acta 49 (2004) 515.
[33] H. Olsson, M. Stromme, L. Nyholm, M. Sjodin, Activation Barriers Provide Insight into the Mechanism of Self-Discharge in Polypyrrole, J. Phys. Chem. C 118 (2014) 29643.

Figure 1. Self-discharge profiles (U *vs* t) of a AC-PTFE/AC-PTFE coin-cell capacitor in 2.0 mol L^{-1} Li_2SO_4 after 3 h potential hold at U_i = 1.0 V (—), 1.2 V (- - -), 1.4 V (···) —·—

and 1.6 V ( ) . Temperature 24 ± 1ºC. The value of cell potential drop after 15 hours is indicated close to each curve.

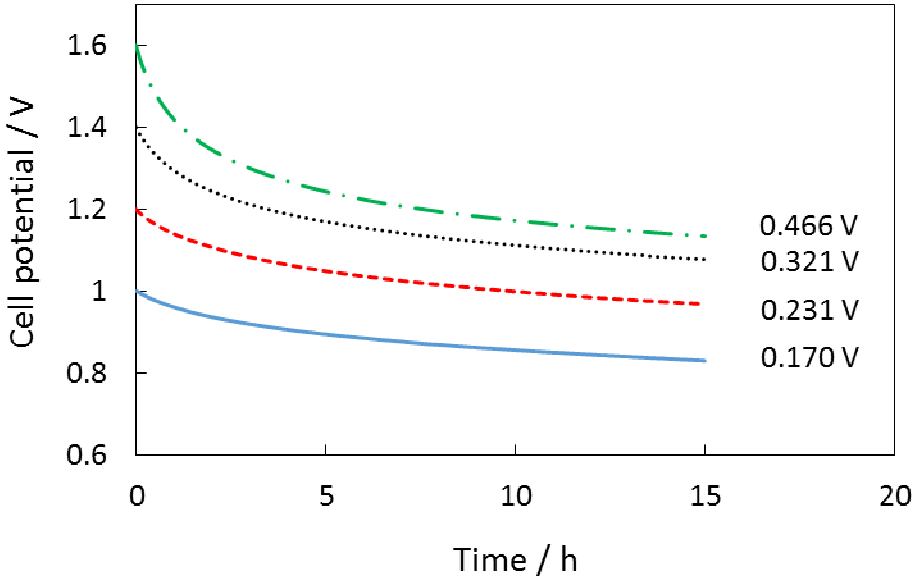

Figure 2. Leakage current of an AC-PTFE/AC-PTFE coin-cell capacitor in 2.0 mol L^{-1} Li_2SO_4 vs floating time for various values of potential hold U_i = 1.0 V (—), 1.2 V (- - -), 1.4 V (···) and 1.6 V (— · —). Temperature 24 ± 1ºC.

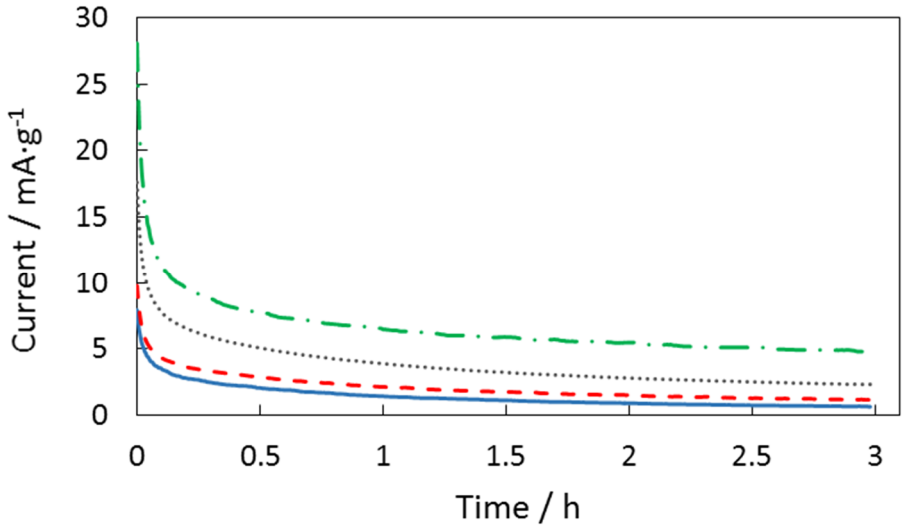

Figure 3. Self-discharge profiles (U *vs* t) of a AC-PTFE/AC-PTFE coin-cell capacitor in 2.0 mol L^{-1} Li_2SO_4 after 3 h potential hold at U_i = 1.0 V (—), 1.2 V (- - -), 1.4 V (···) and 1.6 V (— · —). Temperature 34 ± 1ºC. The value of cell potential drop after 15 hours is indicated close to each curve.

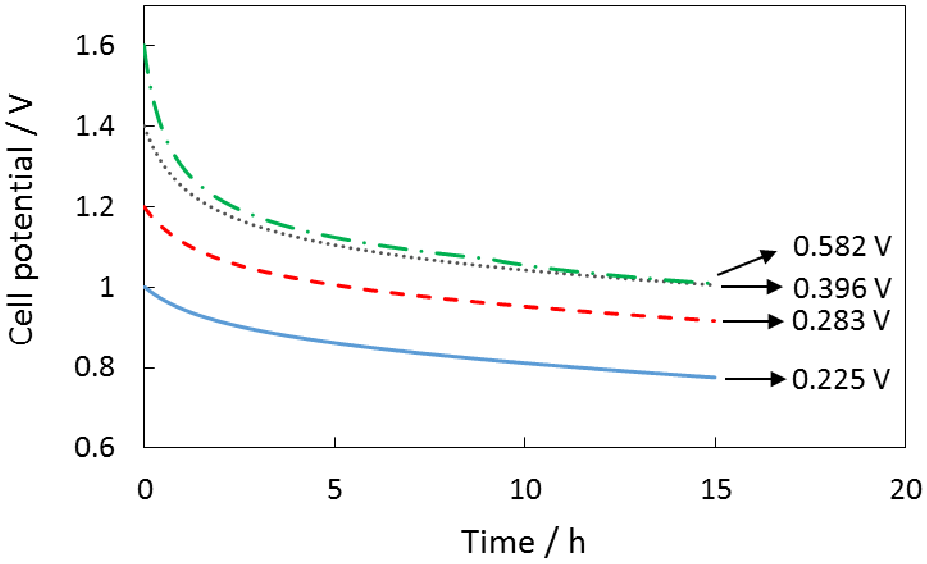

Figure 4. Leakage current of a AC-PTFE/AC-PTFE coin-cell capacitor in 2.0 mol L^{-1} Li_2SO_4 *vs* floating time for various values of potential hold U_i = 1.0 V (—), 1.2 V (- - -), 1.4 V (···) and 1.6 V (— · —). Temperature 34 ± 1ºC.

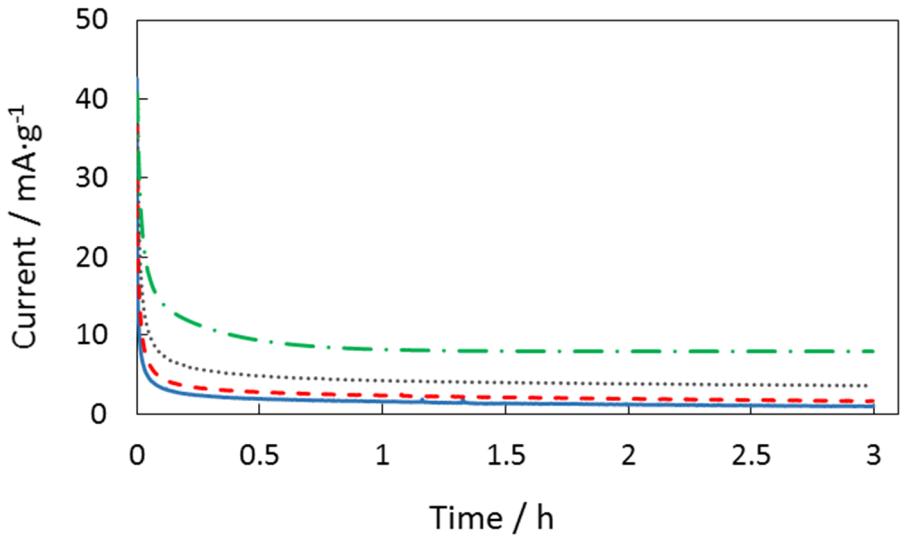

Figure 5. (a) Cell potential *vs* $t^{1/2}$ for an AC-PTFE/AC-PTFE coin cell capacitor in 2.0 mol L^{-1} lithium sulfate after 3 h of potential hold at U_i = 1.0 (—), 1.2 V (- - -), 1.4 (···), and 1.6 V (—·—); (b) Cell potential *vs* ln t for an AC-PTFE/AC-PTFE coin cell capacitor in 2.0 mol L^{-1} lithium sulfate after 3 h of potential hold at U_i = 1.0 (—), 1.2 V (- - -), 1.4 (···), and 1.6 V (—·—). Temperature 34 ± 1ºC.

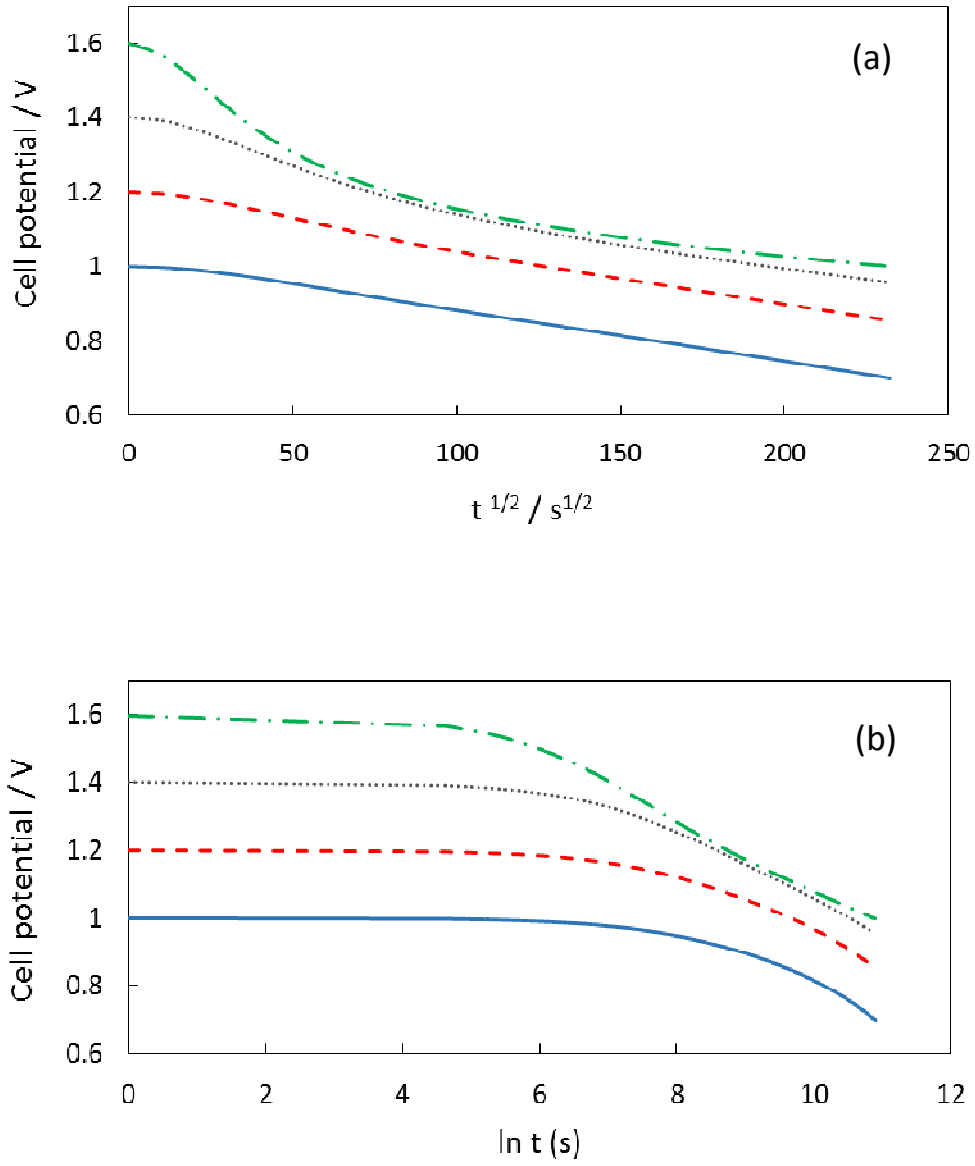

Figure 6. Cell potential (—), positive electrode potential (—), negative electrode potential (—) *vs* time for an AC-PTFE/AC-PTFE capacitor with reference electrode in 2.0 mol L^{-1} lithium sulfate after 3 h of potential hold at U_i = 1.0 and 1.4 V. Temperature 24 ± 1ºC.

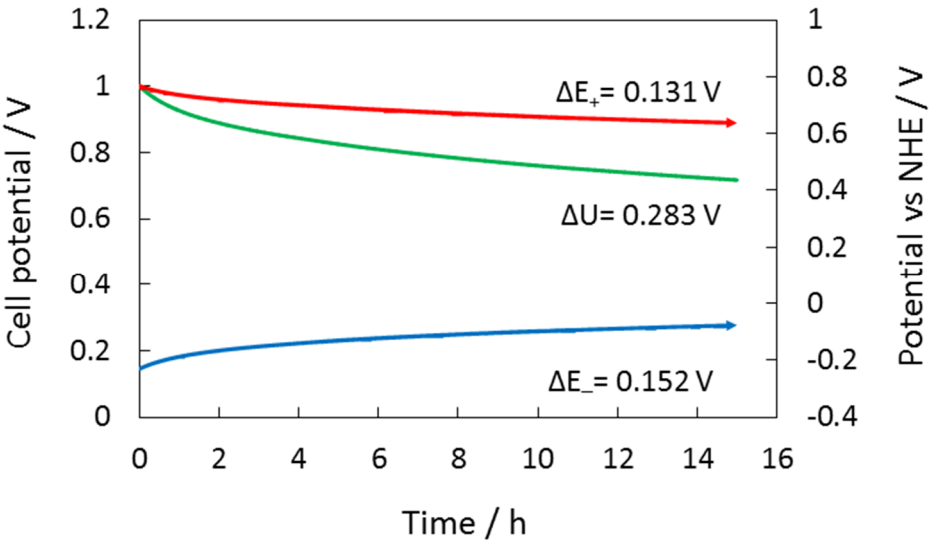

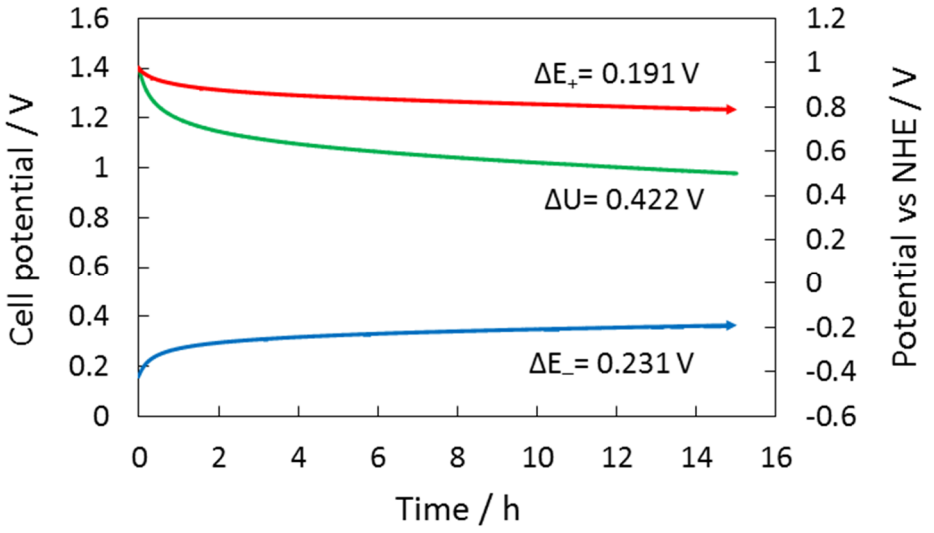

Figure 7. (a) Cell potential, (b) positive electrode potential, (c) negative electrode potential *vs* $t^{1/2}$ for an AC-PTFE/AC-PTFE capacitor with reference electrode in 2.0 mol L^{-1} lithium sulfate after 3 h of potential hold at U_i = 1.0 (—), 1.2 V (- - -), 1.4 (···), and 1.6 V (— · —). Temperature 24 ± 1ºC.

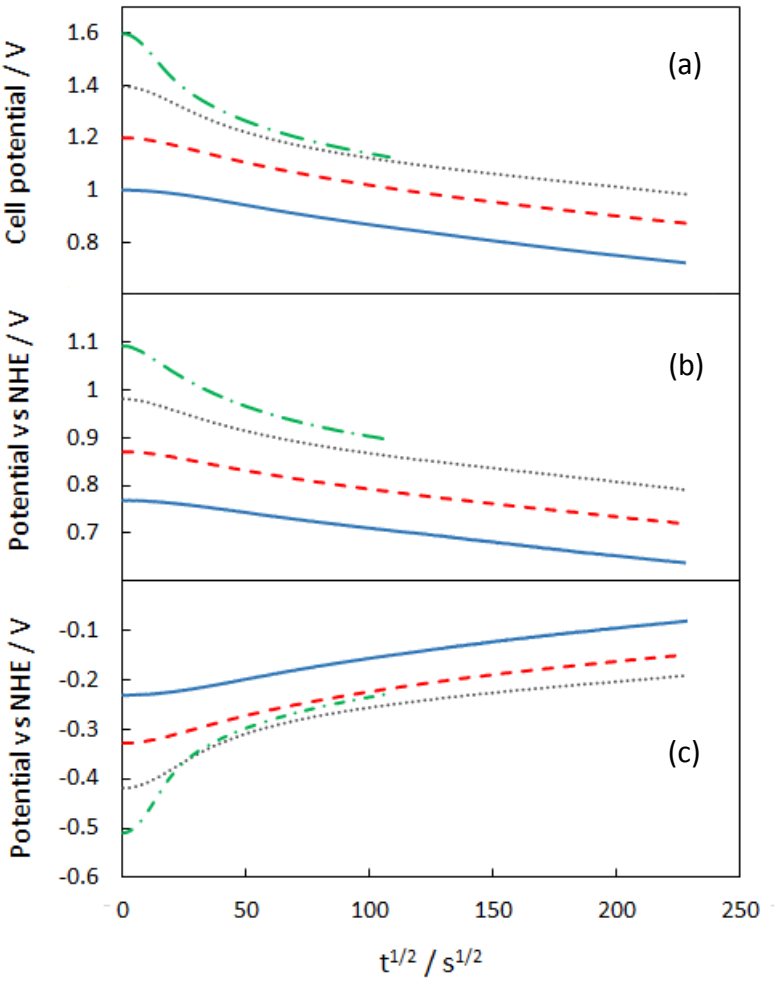

Figure 8. (a) Cell potential, (b) positive electrode potential, (c) negative electrode potential *vs* ln t for an AC-PTFE/AC-PTFE capacitor with reference electrode in 2.0 mol L^{-1} lithium sulfate after 3 h of potential hold at U_i = 1.0 (—), 1.2 V (- - -), 1.4 (···), and 1.6 V (— · —). Temperature 24 ± 1ºC.